Evaluation of Subarachnoid Space Volume Using Segmentation Techniques in MRI Imaging

Kunlun Li

***Abstract*—Magnetic Resonance Imaging (MRI) is a pivotal tool in the detection and analysis of brain diseases, offering detailed insights into neurological structures and functions. This paper conducts an in-depth analysis of processes involved in registration, segmentation, Evans ratio, and subarachnoid space (SAS) volume calculations, as well as the synthesis of T1-weighted (T1w) and T2-weighted (T2w) MRI images. The study begins with a detailed review of the dataset format and its contents, followed by a comparison with previous works to establish contextual relevance. The methodology introduced includes aligning T1w and T2w images to a 1mm MNI space, employing FastSurfer for ventricle segmentation in brain MRI, synthesizing T2w images from existing T1w images using a Cycle Generative Adversarial Network (CycleGAN), and calculating SAS volume in T2-weighted MRI images through segmentation and traditional methods. The paper will provide an evaluation of the employed methods and metrics. Finally, the strengths and limitations of these methods will be discussed, with considerations for improvements by comparing them to the approaches used by other groups.**

***Index Terms*—Magnetic resonance imaging, Registration, Segmentation, Synthesis, Evans Ratio, Subarachnoid Space Volume, CycleGAN, FreeSurfer**

I. Introduction

Magnetic resonance imaging (MRI) is a non-invasive imaging technique renowned for its superior soft tissue contrast and diverse physiological and functional applications [1]. Tailored MRI pulse sequences generate distinct contrasts for the same anatomy: T1-weighted images accentuate the distinction between gray and white matter, while T2-weighted images highlight differences between fluid and cortical tissue. The selection of appropriately weighted images tailored to specific diagnostic needs is crucial. For example, T2-weighted MRI is utilized for detecting cerebral microbleeds, commonly found in small vessel diseases among the elderly [2]. Conversely, T1-weighted MRI is employed to analyze subcortical brain structures for the early detection of neurological disorders, offering a high level of diagnostic accuracy [3].

The Montreal Neurological Institute (MNI) template is widely used in brain structure analysis because it provides a standardized stereotaxic space for neuroimaging studies. This standardization allows for the transformation of images from different subjects into a common space, facilitating direct comparisons and statistical analyses across individual or group studies [4]. Additionally, advanced techniques such as FastSurfer[5], FreeSurfer[6], SLANT[7], and other deep learning models provide accurate segmentation of the lateral ventricle, which aids in measuring the subarachnoid space (SAS) volume [8] and Evans ratio [9], critical metrics for managing patients with neurological conditions.

The remainder of this paper is organized as follows: Section II provides a basic description of the dataset used in this study and reviews prior works that set the theoretical foundation for the methods later employed. Section III details the methods used in this project, the experiments conducted, criteria for evaluation, and the results obtained when these methods were applied to the training data. Section IV evaluates the overall performance of the methods used, discusses their limitations and strengths by comparing results with those from other groups, and considers potential improvements for the project. Finally, the contributions of the team members will also be illustrated.

II. Background

A. Dataset Description

The dataset for this study consists of 50 T1-weighted (T1w) images, 50 T2-weighted (T2w) images, and 2 MNI template images, all stored in gz files and accessible via MIPAV or similar medical imaging software. T1w images, characterized by shorter repetition and echo times, effectively highlight tissues with short T1 relaxation times (e.g., fat), appearing brighter, while tissues with longer T1 times (e.g., water or CSF) appear darker. This contrast facilitates clear differentiation between brain structures: gray matter appears darker than white matter, and cerebrospinal fluid (CSF) is shown as dark. Conversely, T2w images, providing a distinct contrast, make CSF appear very bright, rendering these images particularly useful for identifying fluid-filled lesions. The inclusion of two MNI template images facilitates the registration of T1w and T2w images to a common space, enabling streamlined analysis.

Challenges were evident from the outset of the project. As illustrated in Figures 1, it is clear that some T2-weighted (T2w) images are of suboptimal quality due to prior downsampling, which has resulted in a resolution lower than that of the T1-weighted (T1w) images. Furthermore, the limited size of the dataset presents substantial challenges for effective segmentation and synthesis, impacting the overall ability to achieve precise and reliable outcomes.

B. Prior work on MRI Image Registration

Throughout the years, numerous algorithmic approaches for image registration have been introduced. Initially, registration techniques relied on manually or automatically extracted features to align corresponding points between images [10]. As

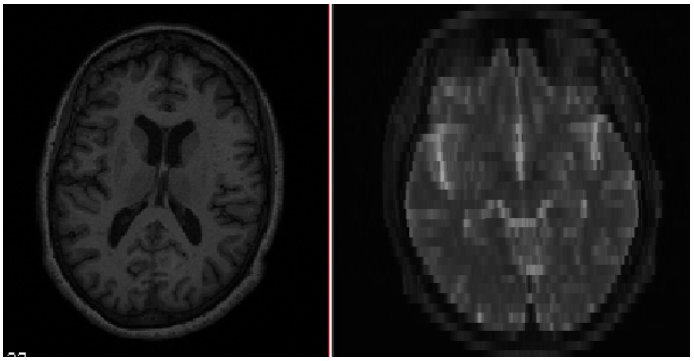

Fig. 1. The T1w(Left) and T2w(Right) MRI from subject40

computational capabilities advanced, intensity-based methods, which leverage complete image data, emerged, significantly improving alignment precision [11]. Furthermore, the advent of deep learning has introduced novel approaches to MRI registration; notably, the use of Generative Adversarial Networks (GANs) for unsupervised registration processes [12].

C. Prior Work on Ventricle Segmentation

Following the registration of images to a common space, ventricle segmentation becomes crucial for measuring the subarachnoid space (SAS) volume. Both traditional methods and machine learning approaches have been employed to address this challenge. Research has delved into the automatic segmentation of the brain in MRI, specifically targeting the ventricular system. It describes a dual-phase technique that combines initial pixel-level segmentation with subsequent template matching for ventricle identification [13]. With the evolution of deep learning, sophisticated methods such as FreeSurfer [6], FastSurfer [5], and SLANT [7] have been introduced. These techniques not only utilize geometric and statistical information from the cortical surface and tissue classes but also leverage 3D volumetric convolutional neural networks for comprehensive brain segmentation.

D. Prior Work on MRI image synthesis

Prior research has explored the synthesis of synthetic MRI images using advanced techniques such as Generative Adversarial Networks (GANs) and Convolutional Neural Networks (CNNs) [14]. In the GAN framework, the generator produces images mimicking authentic MRI scans from random noise, while the discriminator assesses them alongside actual scans to differentiate between the real and synthetic. With ongoing training, the generator enhances its capability to create images that increasingly fool the discriminator. Conversely, CNN-based methods learn from the features of existing MRI scans to construct new images. They iteratively adjust through convolutional layers, synthesizing images that closely resemble the specific attributes of genuine scans. Another proposed approach is to use CycleGANs [15],as illustration in the figure 2, the two types of Generative Adversarial Networks (GANs) are trained simultaneously to convert images from one domain to another and vice versa.

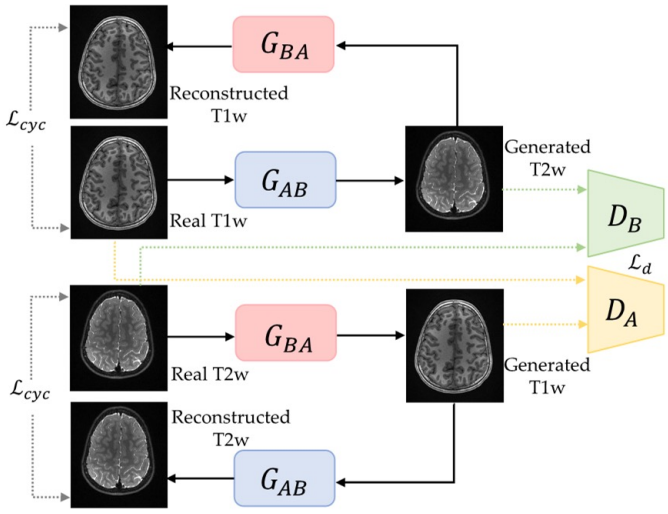

Fig. 2. The Architecture of CycleGANs

III. Methods and Results

A. Registration of MRI Image in FSL

In Task A, the registration process utilizes the FSL (FMRIB Software Library), a comprehensive toolset for MRI analysis. Initially, linear registration is employed with the Montreal Neurological Institute (MNI) standard brain serving as the reference image, and the T1-weighted (T1w) MRI as the input. This step involves adjusting the orientation of the T1w image to align precisely with the MNI template. The correlation ratio is utilized as the cost function to optimize this alignment, providing a crucial measure of how well the intensities of the two images correlate within the overlapping region.

For the interpolation of images, a Nearest Neighbour method is chosen for its ability to ensure a smooth and continuous transformation, which is essential for maintaining the integrity of the image data throughout the transformation process. After the successful registration of the T1w image to the MNI space, this registered T1w image is then used as the reference for registering the T2-weighted (T2w) MRI images. The T2w images are inputted, and the same linear registration process is applied. Using the registered T1w image as the reference ensures that the T2w images are aligned within the same anatomical space, thereby facilitating subsequent analyses.

Given the critical need to preserve the geometric integrity of the images during the registration process, the interpolation has been implemented. This method aids in maintaining the continuity and smoothness of the images, which is beneficial for preserving their geometric accuracy. Additionally, the use of linear registration with a correlation ratio as the cost function helps to preserve the original geometry of the brain structures effectively.

This methodical approach to registration ensures that both T1w and T2w images are consistently aligned with the high-resolution standard space of the MNI template, thereby en-

hancing the reliability and validity of any subsequent neuroimaging analyses.

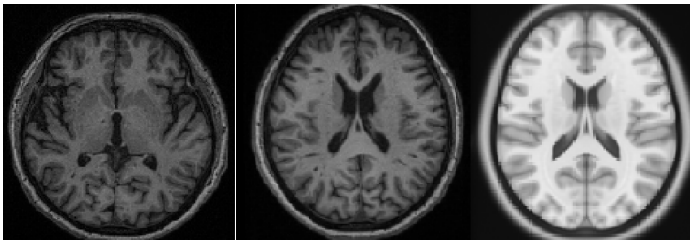

Fig. 3. The T1w MRI from Test01 before(left), after(middle) Registration and MNI Template(right)

B. FreeSurfer based Ventricle Segmentation and Evans Ratio

After aligning all T1-weighted (T1w) and T2-weighted (T2w) images to the same MNI template, we utilize FastSurfer [5] within the Windows Subsystem for Linux (WSL) environment to perform brain segmentation on the registered images. This process yields comprehensive brain segmentation results. The segmented outcomes can then be visualized using Freeview [5], which allows for the inspection of the output volume files.

Given that the Evans Ratio is defined by the maximum width of the frontal horns of the lateral ventricles relative to the maximal internal diameter of the skull at the same axial level, it is necessary to specifically extract the lateral ventricles and brain mask from the axial slices. This extraction is facilitated by the save volume tool within Freeview.

Subsequent to the segmentation, basic image processing operations such as rotation and flipping are applied to the segmented ventricles and brain mask to ensure they are properly aligned with the source images. The results are shown in the figure 4. Finally, a straightforward algorithm has been

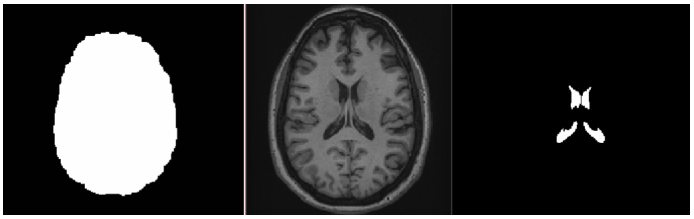

Fig. 4. The Segmentation Result from FastSurfer, from Left to Right are the Brain Mask, Source Image, Lateral Ventricle

developed to process these segmented images. This algorithm calculates the Evans Ratio by first summing up the ventricles and brain mask arrays column-wise across the axial slices. It then determines the Evans Ratio by dividing the maximum width of the lateral ventricles by the maximum width of the brain, providing a quantitative measure of ventricular enlargement.

C. CycleGAN based MRI Image Synthesis

If we are more interested in the fluids of the brain, we prefer to look at T2w images since the fluid appears brighter. Therefore, computing SAS volume is best done on the T2w image. The CycleGAN is chosen to produce T2w image from available T1w image in some case that the T2w has very low quality. The method will include Preprocessing, Model prediction and Pose-processing steps.

The preprocessing stage involved converting MRI data from NIfTI format to PNG, segmenting the files into individual slices using the mri_image_process code. This step ensured ease of manipulation and consistent input preparation. Subsequently, image manipulation techniques such as rotations and cropping were applied to align and size the MRI slices appropriately, setting the stage for effective model training and synthesis.

In the prediction part, a pre-trained CycleGAN, a deep learning model adept at image-to-image translation from unpaired datasets, was utilized to synthesize T2-weighted (T2w) images from T1-weighted (T1w) inputs. This model is particularly suitable for medical imaging contexts where paired T1w and T2w images of the same slice are often unavailable.

In the training part, the model was tailored to the unique requirements of MRI image characteristics, such as varying tissue contrasts, through a training regimen adapted from similar applications in brain MRI analysis. Following training, the model was employed to generate T2w slices from the preprocessed T1w slices, facilitating the creation of high-quality imaging data where original T2w images were insufficient.

Finally, the synthetic T2w slices underwent post-processing to ensure they matched the original dimensions and orientations of the T1w slices. This process was critical to maintain spatial consistency. The reassembly of these slices into a cohesive 3D NIfTI format was achieved using saved affine matrices, preserving the anatomical accuracy of the images.

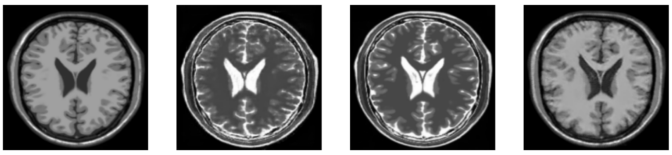

Fig. 5. The Result of Synthesis after Training 200 Epochs, from Left to Right are: Input T1w MRI, T1w to T2w Converted, Input T2w MRI, T2w to T1w Converted

D. SAS Volume Measurement

The extraction of the subarachnoid space (SAS) began with k-means clustering to segment the initial region, effectively isolating the SAS based on pixel intensities. This was followed by a region-growing algorithm to enhance the delineation accuracy by including adjacent pixels of similar intensities. To refine this segmentation, mathematical morphology operations were applied to smooth edges and reduce noise. The process concluded with a second round of region growing and morphological operations to further sharpen and define the SAS boundaries, ensuring precise and clean segmentation suitable for detailed neurological analysis.

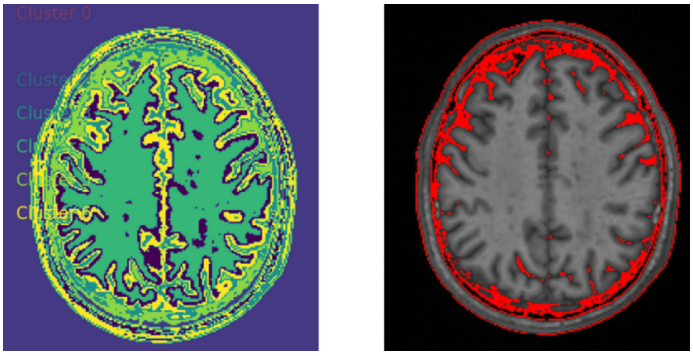

Fig. 6. The Result of Applied K-means Clustering to the source image(left) and the Inital SAS Segmentation Mask(right)

E. Evaluation

Registration: As we lack ground truth data for subjects post-registration into the MNI template, visual inspection will be used to assess the alignment of structures within overlaid images. This qualitative approach will help evaluate the accuracy of the registration by examining the congruency of anatomical features across the images.

Segmentation and Evans Ratio Measurement: The accuracy of the ventricle segmentation and the subsequent Evans Ratio calculation will be validated through comparisons with results from multiple established algorithms. Given the absence of a definitive ground truth for the Evans Ratio, its evaluation will primarily rely on the judgment of the teaching staff. Nonetheless, an expected range for the Evans Ratio, sourced from reputable online medical sources, will provide a preliminary benchmark to assess the plausibility of our results.

- 0.20-0.25: normal
- 0.25-0.30: possible or early ventriculomegaly
- >0.30: ventriculomegaly

Fig. 7. The expected range for the Evans Ratio found on the Radiopaedia

Synthesis and SAS Volume Calculation: The quality of the synthesized T2-weighted images will be evaluated by comparing them against the original T2w images they are intended to replicate. For the SAS volume, we will use an anticipated range obtained from internet research as a reference. As found, the normal range for cerebrospinal fluid (CSF) volume, which largely occupies the subarachnoid space, is typically cited as around 125 mL in the intracranial subarachnoid spaces for adults. This benchmark will help confirm whether our results fall within a reasonable spectrum.

IV. Discussion and Conclusion

During the demonstration day, we got the performance of our method on the test data, which presented in Figure 9.

It was evident that our method underperformed, as indicated by the high Mean Squared Error (MSE) values in Tasks A and C. However, the demonstration allowed us to recognize

93383.1243	0.2526	n/a	3343.195

Fig. 8. Evaluation Result from Demo Day, from Left to Right is Task A, Task B, Task C(Synthetic T2w), Task C(SAS Volume), all under Mean Square Error(MSE) metrics

the limitations of our approach and identify potential improvements.

Registration: Despite the high MSE observed across all groups, we learned valuable lessons from our peers. For future improvements, we could explore alternative cost functions such as Mutual Information or Least Squares and consider other interpolation methods like B-Spline, which some groups used successfully.

Segmentation: Our MSE was slightly higher than that of the leading group (approximately 0.15). Given that we, like the more successful groups, utilized FastSurfer for segmentation, the fundamental structure of our method appears sound. The likely source of error may stem from our selection of the external brain mask rather than an internal one. Additionally, we should focus on preserving only the frontal horns of the lateral ventricle for more accurate measurements, as our current approach mistakenly prioritizes the wider temporal horns.

T2w Synthesis: Unfortunately, due to incorrect output sizes, we were unable to evaluate our CycleGAN's performance. Future iterations could benefit from exploring regression models or employing a U-net architecture for synthesis, as observed in other groups' successful strategies.

SAS Volume Calculation: Our initial approach using region-based methods yielded poor results. Inspired by successful strategies from other groups, we plan to adopt the mask generated by FastSurfer applied directly to the source images for more accurate SAS volume estimations.

In the whole MRI project. I was responsible for using FreeSurfer for ventricle segmentation and Evans Ratio calculations during both the development and testing phases. Boshen Pan handled the MNI template registration, providing the registered images needed for my segmentation tasks. Peiqi Shi spearheaded the T2w image synthesis using CycleGANs in Task C. Langxin Yang employed region-growing methods for estimating the SAS volume.

Throughout the project, our team maintained close communication, sharing ideas and jointly addressing challenges during the method development and testing phases. This collaborative effort was extended during the evaluation, where we actively discussed and analyzed each task's outcomes.

Reflecting on the demonstration day, we critiqued our model's overall performance and contemplated potential enhancements by comparing our methods with those employed by other groups. This project was not only educational in terms of medical image analysis but also a valuable collaborative experience. Working with my teammates on real-world problems has provided me with invaluable insights and experiences that will undoubtedly aid my further pursuits in this field.

REFERENCES

[1] M. Ghadimi and A. Sapra, "Magnetic Resonance Imaging (MRI), Contraindications," PubMed, May 08, 2022. https://www.ncbi.nlm.nih.gov/books/NBK551669/

[2] M. Y. Tang, T. W. Chen, X. M. Zhang, and X. H. Huang, "GRE T2-Weighted MRI: Principles and Clinical Applications," BioMed Research International, Apr. 16, 2014. https://www.hindawi.com/journals/bmri/2014/312142/

[3] S. Chakraborty, S. Aich, and H.-C. Kim, "Detection of Parkinson's Disease from 3T T1 Weighted MRI Scans Using 3D Convolutional Neural Network," Diagnostics, vol. 10, no. 6, p. 402, Jun. 2020, doi: https://doi.org/10.3390/diagnostics10060402.

[4] M. Dadar, A. L. Manera, V. S. Fonov, S. Ducharme, and D. L. Collins, "MNI-FTD templates, unbiased average templates of frontotemporal dementia variants," Scientific Data, vol. 8, no. 1, Aug. 2021, doi: https://doi.org/10.1038/s41597-021-01007-5.

[5] L. Henschel, S. Conjeti, S. Estrada, K. Diers, B. Fischl, and M. Reuter, "FastSurfer - A fast and accurate deep learning based neuroimaging pipeline," NeuroImage, vol. 219, p. 117012, Oct. 2020, doi: https://doi.org/10.1016/j.neuroimage.2020.117012.

[6] B. Fischl, "FreeSurfer," NeuroImage, vol. 62, no. 2, pp. 774–781, Aug. 2012, doi: https://doi.org/10.1016/j.neuroimage.2012.01.021.

[7] Y. Xiong, Y. Huo, J. Wang, L. T. Davis, M. McHugo, and B. A. Landman, "Reproducibility Evaluation of SLANT Whole Brain Segmentation Across Clinical Magnetic Resonance Imaging Protocols," Proceedings of SPIE–the International Society for Optical Engineering, vol. 10949, p. 109492V, Feb. 2019, doi: https://doi.org/10.1117/12.2512561.

[8] R. G. Steen, R. M. Hamer, and J. A. Lieberman, "Measuring Brain Volume by MR Imaging: Impact of Measurement Precision and Natural Variation on Sample Size Requirements," American Journal of Neuroradiology, vol. 28, no. 6, pp. 1119–1125, Jun. 2007, doi: https://doi.org/10.3174/ajnr.A0537.

[9] X. Zhou and J. Xia, "Application of Evans Index in Normal Pressure Hydrocephalus Patients: A Mini Review," Frontiers in Aging Neuroscience, vol. 13, Jan. 2022, doi: https://doi.org/10.3389/fnagi.2021.783092.

[10] B. Zitová and J. Flusser, "Image registration methods: a survey," Image and Vision Computing, vol. 21, no. 11, pp. 977–1000, Oct. 2003

[11] C.-L. Cocianu, C. R. Uscatu, and A. D. Stan, "Evolutionary Image Registration: A Review," Sensors, vol. 23, no. 2, p. 967, Jan. 2023

[12] Bharati S, Mondal M, Podder P, Prasath VB. Deep learning for medical image registration: A comprehensive review. arXiv preprint arXiv:2204.11341. 2022 Apr 24

[13] M. S. Atkins and B. T. Mackiewich, "Fully automatic segmentation of the brain in MRI," IEEE Transactions on Medical Imaging, vol. 17, no. 1, pp. 98–107, 1998, doi: https://doi.org/10.1109/42.668699.

[14] H. Zhang, H. Li, J. R. Dillman, N. A. Parikh, and L. He, "Multi-Contrast MRI Image Synthesis Using Switchable Cycle-Consistent Generative Adversarial Networks," Diagnostics, vol. 12, no. 4, p. 816, Mar. 2022

[15] H. Zhang, H. Li, J. R. Dillman, N. A. Parikh, and L. He, "Multi-Contrast MRI Image Synthesis Using Switchable Cycle-Consistent Generative Adversarial Networks," Diagnostics, vol. 12, no. 4, p. 816, Mar. 2022, doi: https://doi.org/10.3390/diagnostics12040816.

APPENDIX

Here is the code for our MRI project Project Documentation.